



Time-variations of wave energy and forecasting power availability at a site in Fiji using time-series, regression and ANN techniques

Avikesh Kumar, Gabriele Bulivou, Mohammed Rafiuddin Ahmed & Mohammad Golam M. Khan

To cite this article: Avikesh Kumar, Gabriele Bulivou, Mohammed Rafiuddin Ahmed & Mohammad Golam M. Khan (02 Sep 2024): Time-variations of wave energy and forecasting power availability at a site in Fiji using time-series, regression and ANN techniques, Journal of the Royal Society of New Zealand, DOI: [10.1080/03036758.2024.2395910](https://doi.org/10.1080/03036758.2024.2395910)

To link to this article: <https://doi.org/10.1080/03036758.2024.2395910>



Published online: 02 Sep 2024.



Submit your article to this journal [↗](#)



View related articles [↗](#)




View Crossmark data [↗](#)

RESEARCH ARTICLE



Time-variations of wave energy and forecasting power availability at a site in Fiji using time-series, regression and ANN techniques

Avikesh Kumar, Gabiriele Bulivou, Mohammed Rafiuddin Ahmed  and Mohammad Golam M. Khan

School of Information Technology, Engineering, Mathematics & Physics, The University of the South Pacific, Suva, Fiji

ABSTRACT

Recently, there has been a shift in the global energy landscape to move to reliable, clean, and eco-friendly renewable energy sources to address global issues such as climate change and greenhouse gas emissions. One such energy source is wave energy; researchers attempt to develop models that can accurately forecast the availability of wave energy as an alternative energy source. In this paper, an Artificial Neural Network (ANN) model along with statistical models such as time series models, and regression models are proposed for forecasting wave energy at a site in Fiji using the wave height and wave period as the independent variables. The performance of the proposed models developed is compared using Mean Squared Error (MSE), Root Mean Squared Error (RMSE), Mean Absolute Error (MAE), Mean Absolute Percentage Error (MAPE), and the goodness-of-fit (R^2) value. The proposed model is then further benchmarked with the naïve model. The empirical results reveal that the proposed ANN model outclassed all the other models and was more efficient and accurate in forecasting wave energy than the regression and time series models. By accurate wave modelling and by incorporating impedance matching, maximum power generation can be achieved.

ARTICLE HISTORY

Received 27 February 2024
Accepted 20 August 2024

HANDLING EDITOR

Mathieu Sellier

KEYWORDS

Wave energy; forecasting; time series models; regression model; artificial neural network; marine renewable energy

Introduction

Forecasting plays a key role in providing realistic energy figures, assisting policymakers in making informed decisions about using different renewable energy sources. This is crucial as we transition into an era where alternative energy sources aim to provide cleaner energy while meeting rapidly increasing demands (Thomas et al. 2015). As renewable energy sources become more cost-competitive against oil-generated electricity, more nations are considering these substitutes to combat climate change (IEA 2020; Posterari and Waseda 2022). Twidell and Weir (2015) state that renewable energy supplies are much more compatible with sustainable development than fossil fuels, considering their resource limitations and environmental impacts.

The International Energy Agency (IEA) predicted a 7% growth in renewable energy for electricity by 2020 and that by 2050, 90% of the world's electricity would come from renewable sources (IRENA 2017).

In many countries, solar, hydro, and wind energy are commonly considered alternative energy sources (IPCC 2014). However, there is a need to explore all forms of renewable energy for a sustainable future (IRENA 2017). The Pacific Island Countries (PICs) have heavily relied on fossil fuels over the years, causing environmental and economic concerns due to global instability (Posterari and Waseda 2022). While wind, solar Photovoltaic (PV), and hydro sources have proven efficient and reliable for Fiji and other PICs, wave energy presents a significant untapped potential. Many researchers suggest that wave energy can dominate other energy sources since waves are constantly present. Reikard et al. (2015) highlighted significant wave energy potential along the coasts of Washington and Oregon, and Ram et al. (2014), cited considerable wave power potential in the USA, China, and India. Ali et al. (2020) claim that Australia has a high potential for ocean energy generation, which could reduce greenhouse emissions by 26–28% by 2030. The European Commission is also targeting substantial ocean energy installations by 2025, 2030, and 2050 (OES 2022). Given the strong commitment from IEA countries, wave energy can diversify energy supplies in PICs and potentially compete with other energy sources.

Fiji, with a sea-to-land area ratio of 70 and a coastline of 1129 km, has a wave power potential of 29 GW, of which only 0.5% is enough to meet the energy requirements of the country (Kumar et al. 2020). Wave energy research is not new to Fiji; the South Pacific Geosciences Commission (SOPAC) initiated a wave energy resource assessment programme in 1987, followed by the Norwegian Government through the Norwegian Agency for International Development (NORAD) from 1987 to 1995 (Ram et al. 2014). An assessment in 2015 revealed that Fiji has a mean wave energy flux of 24 kW/m per metre (kW/m) with a theoretical annual energy output of 1,017 MWh (Cyprien et al. 2015). Fiji lies in a tropical zone where cyclones and weather patterns pose risks to wave energy devices. Therefore, more research was conducted near shore, considering that nearshore wave energy devices are less expensive, easier to maintain, and have a longer life than offshore devices (Ram et al. 2014).

Good modelling of wave energy helps in model-based control design that can be used for performance improvement of wave energy harvesters (Coe et al. 2021). Successful applications of Artificial Neural Networks (ANN) in forecasting wave energy in various regions (Mandal and Prabakaran 2010; Hadadpour et al. 2014; Kashikar and Mane 2014; Li et al. 2023) provide assurance that wave power could be viable for countries heavily reliant on fossil fuels. Wave power generation also helps to prevent coastal erosion and to address climate change impacts on near-shore communities.

Given the environmental, economic, and social challenges associated with harvesting wave energy, a feasibility study is crucial before wave energy can be accepted as a viable substitute for other forms of energy (Felix et al. 2019). Therefore, this study aims to develop and compare forecasting models, including time series, regression, and ANN models, to identify the optimum model for wave energy at a site in Fiji.

The novel aspect of this research is the contribution to the advancement in the field of wave energy forecasting by introducing new methodologies and suggesting future research avenues. The research introduces an Artificial Neural Network (ANN) model

specifically for forecasting wave energy at a site in Fiji, which can outperform traditional regression and time-series models. It specifically targets wave energy forecasting in Fiji, a region where wave energy potential is underexplored and highlights the possibility of extending the developed forecasting models to other Pacific Island Countries (PICs). Moreover, the research integrated multiple variables using wave height and wave period as independent variables to forecast wave power, providing a methodological contribution to wave energy forecasting, which can improve the accuracy of forecasting models.

Section ‘Background’ of the paper discusses the related work, while Section ‘Methodology’ describes the methodology used in developing the forecasting models. The results and discussions are presented in Sections ‘Results’ and ‘Discussion’, and the conclusions are drawn in Section ‘Conclusion’.

Background

The main objective of any forecasting model is to minimise uncertainties and maximise its reliability and sustainability as results are predicted from past to present and into the future. In this section, different forecasting models such as time series, regression, naïve, and ANN models are discussed.

Time series model

Time series models focus on analysing data that exhibit trends, cycles, and seasonal patterns with asymmetrical components (Barak and Sadegh 2016; Kumar et al. 2020). These models require data recorded at fixed and constant intervals (Kimata 2016). According to Kalekar (2004), time series data consist of a combination of patterns and random errors, with the goal being to separate these components by understanding trends, seasonal factors, and long-term variations. Four common time series models are the exponential smoothing method, Holt-Winters additive method, Holt-Winters multiplicative method, and the Autoregressive Integrated Moving Average (ARIMA) model.

Exponential smoothing method

The exponential smoothing technique, introduced by Holt in 1957, has evolved to incorporate trends and seasonal components in the data (Dumicic et al. 2008). This method ‘smooths out’ a discrete-time data series using a moving average technique (Hatalis et al. 2014), with recent observations weighted more heavily than older ones (Kalekar 2004). The basic exponential smoothing formula (Winston 2003; Kimata 2016; Kumar et al. 2020) is

$$A_t = A_{t-1} - \alpha e_t \quad (1)$$

where A_t is the forecast value at time t , A_{t-1} is the forecast value at time $t-1$, α is the smoothing constant (0–1), and e_t is the forecast error at time t , used to update the next period’s forecast. A higher α value makes the model more sensitive to recent data, while a lower α value biases it towards historical data. This method is used for short-term forecasting of data without trends or seasonality, such as inventory levels or daily sales figures (Ensafi et al. 2022).

The single exponential model was later modified to account for trends, resulting in the double exponential smoothing model (Kalekar 2004; Dumicic et al. 2008; Kimata 2016). This model updates both the level and the trend:

$$A_t = \alpha x_t + (1 - \alpha)A_{t-1} \quad (2)$$

where A_t is the forecast value at time t , α is the smoothing constant, x_t is the observed value at time t , and A_{t-1} is the previous forecast value. This model is applied to data with trends but no seasonality, and is useful for forecasting data such as retail sales (Ensafi et al. 2022).

Holt-Winter (HW) additive method

The HW additive method, proposed in the 1960s, extends exponential smoothing to capture linear trends and additive seasonality (Tirket et al. 2017). It is suitable for data with a constant seasonal variation (Pongdatu and Putra 2018; Razali et al. 2018). The HW additive model has the form:

$$x_t = a + bt + \varepsilon_t \quad (3)$$

where x_t is the observation at time t , a is the base level at the beginning of time t , b is the per-period trend, and ε_t is the error term for period t . This method is applied to data with linear trends and constant seasonal patterns (Koehler et al. 2001) and is useful in retail sales forecasting with predictable seasonal effects (Tratar 2014), and even forecasting fibre production (Pleños 2022).

Holt-Winters (HW) multiplicative method

The HW multiplicative method further extends the HW additive method, suitable for data with seasonal variation proportional to the series level (Kumar et al. 2020) such as electricity demand influenced by seasonal temperature changes (Rajbhandari et al. 2021). The model is expressed as:

$$x_t = ab^t \varepsilon_t \quad (4)$$

where x_t is the observed value at time t , a is the level component representing the baseline values of the series, b^t is the trend component capturing the percentage growth at time t , and ε_t is the random error factor with a mean of 1, which ensures that the errors do not systematically skew the multiplicative structure of the model.

Autoregressive integrated moving average model (ARIMA)

The ARIMA model, also known as the Box-Jenkins model, is widely used for short-range forecasting by capturing autocorrelations and controlling noise and seasonal effects (Barak and Sadegh 2016; Ozturk and Ozturk 2018). An ARIMA (p, d, q) model comprises three parameters; p is the number of autoregressive terms, d is the number of non-seasonal differencing and q is the number of lagged forecast errors in the equation (Kavasseri and Seetharam 2009; Barak and Sadegh 2016; Arzu 2017). An ARIMA model has a form:

$$y_t = c + a_1 y_{t-1} + \dots + a_p y_{t-p} + u_t + m_1 u_{t-1} + \dots + m_q u_{t-q} \quad (5)$$

where c is a constant that represents the mean of the series and it shows that the data values have been replaced with difference values of order d to obtain stationary data, $a_1 \dots a_p$

are the coefficients of the autoregressive (AR) terms capturing the relationship between the current value and its past values up to lag p , while $m_1 \dots m_q$ are the coefficients of the moving average (MA) terms capturing the relationship between the current value and past error terms up to lag q . Both coefficients $a_1 \dots a_p$ and $m_1 \dots m_q$ are found through statistical estimation methods such as the Maximum Likelihood Estimation (MLE) or Least Squares Estimation (LSE). y_t is the actual data value of the d^{th} difference at time t , y_{t-1} is the data value at time $t-1$, u_t is the random error at time t representing random fluctuations, u_{t-1} is the random error at time $t-1$, p is the autoregressive order and q is the moving average order of the model. This model is used for forecasting by capturing both the persistence of past values and the influence of past errors, common in economic and financial time series forecasting, and more recently in forecasting international migration (Tolesh and Biloshchytska 2024).

Regression models

Regression models are good at predicting the dependent variable given that one or more independent variables are known. It can be either through a linear or a nonlinear relationship between the dependent variable and independent variables.

Multiple linear regression models

Multiple Linear Regression (MLR) is a statistical technique that can formulate a linear relationship between variables by studying the correlation between independent and dependent variables (Uyanık and Güler 2013). An MLR model as defined by Kumar et al. (2020), Al Khatip (2011), Uyanık and Güler (2013) is

$$Y = \beta_0 + \beta_1x_1 + \beta_2x_2 + \dots + \beta_kx_k + \varepsilon \tag{6}$$

where Y is the dependent variable which is the power being generated, x_1, x_2, \dots, x_k , the independent variables, $\beta_0, \beta_1, \dots, \beta_k$, the regression coefficients, and ε , the error term. The performance and robustness of the resulting multiple linear regression model are based on its linearity test, normality test, independence test, and homoscedasticity test which will be discussed in the methodology.

Nonlinear regression models

Data collected in an open environment where there is a lack of control over some factors usually exhibits nonlinear relationships between variables. To cater for such cases, data transformation is important. Some commonly used transformations are adding constants, square roots, logarithmic scales, reflections, trigonometric transformations, and so on, and can be easily obtained using the Box–Cox transformation (Osborne 2010). Box–Cox transformation normalises data which is required for determining the correlation between variables and eventually improves the performance of the model compared to using data that is not normalised. It transforms the dependent variable y according to:

$$\begin{cases} \frac{y^\lambda - 1}{\lambda} & \text{if } \lambda \neq 0 \\ \log(y) & \text{if } \lambda = 0 \end{cases} \tag{7}$$

where λ is a parameter estimated with some statistical software during model fitting. Applying this transformation can help address issues of heteroscedasticity and nonlinearity, leading to more reliable and interpretable model results.

Naïve method of forecasting

The naïve forecasting model is a simple benchmark model that is used to compare the performance of all other forecasting models. The naïve forecasting model assumes that the reading of the next period will be the same as its preceding period.

$$A_{t+1} = A_t \quad (8)$$

where A_{t+1} is the forecast for the next period, A_t is the actual value at the current period, t is the period, and $t + 1$ is the next period.

A naïve model can be categorised into a random walk model or a seasonal random walk model. A random walk model just uses the last observation as the future forecast while a seasonal random walk model takes the forecast values from the previous year's actual value. In real-world applications, this method is not predominantly used since data fluctuates over time, making it less reliable for accurate predictions.

Artificial neural network models

ANN is a common, accurate, and widely used forecasting technique for many diverse applications. It is a mathematical model for predicting systems output inspired by the structure and function of a human biological neural network (Qiokata and Khan 2015). ANN is capable of explaining and solving complex, highly nonlinear functions synthesis, which is hard to express mathematically (Kumar et al. 2020). It can also perform with high speed of evaluation, and robustness and most importantly, is adaptive to changes in the data sets (Vimala et al. 2014).

Many researchers have used ANN models to predict wave parameters, which are wave height, wave period, and wave power (Makarynskyy et al. 2002; Rao and Mandal 2005; Mandal and Prabakaran 2010; Asma et al. 2012; Hadadpour et al. 2014; Kumar et al. 2020). Reikard (2013) when predicting wave parameters in the Atlantic Ocean, the Pacific Ocean, and the Gulf of Mexico suggested that statistical models performed better when forecasting power in the first few hours, while the large-scale physics models were better in forecasting over longer-term horizons. Reikard et al. (2015) initially researched four locations in the Pacific Ocean and made similar conclusions when predicting the wave parameters. Moreover, Hadadpour et al. (2014) forecasted wave energy at the Caspian Sea using ANN and for comparison purposes, wave parameters were separately forecasted. They concluded that forecasting parameters separately and then using a formula to find wave power provided more accurate results than forecasting wave power directly for a short period. According to Contreras et al. (2003), a three-layer ANN with a backpropagation model was successfully used for the Victorian electricity market recording a daily average error of around 15%. Vimala et al. (2014) used the ANN technique to forecast the significant wave height with a leading time of 3, 6, 12, and 24 h in the Bay of Bengal and stated very accurate results based on different error measurements used. Bandyopadhyay and Chattopadhyay

(2007) compared the performance of the ANN model with the MLR model while forecasting total Ozone concentration over Arosa, Switzerland, and claimed that ANN out-classed the MLR model based on different evaluators used.

Multi-layer perceptron model is an ANN model that is commonly used which can handle nonlinear systems without making many prior assumptions about the problem (Shen 2024). This model effectively captures complex relationships within the data through multiple layers of interconnected neurones, which allows it to approximate any continuous function given sufficient hidden units and data. An ANN model consists of three important components: the structure, the training algorithm, and the transfer function (Kimata 2016). Its structure consists of the input layer, the hidden layer, and the output layer. From the input layer, the input neurones are passed through some hidden layers where reasonable weights are attached after which the output is obtained by use of a transfer function (Palchak 2012). The structure is such that it allows multiple mapping between neurones so that the required goal is met (Kumar et al. 2020). Literature suggests that there is no fixed algorithm to achieve the optimum structure of a model. One can only achieve this through the trial-and-error method. The optimum number of layers, nodes, and transfer functions will certainly allow the network to capture a distinguished and complicated mapping (linear or nonlinear) between variables (Hsu and Chen 2003; Palchak 2012). Once the targeted output is achieved, a training/learning algorithm is deployed to further allow the model to converge to the desired accuracy by readjusting the attached weights. Figure 1 displays the general structure of an ANN model.

A basic working multi-layer perceptron model can also be illustrated with fundamental mathematical notations. Assuming a total Q sets of training data are available, inputs $\{o_1, o_2, \dots, o_a\}$ are passed through the hidden layer; the model is trained to get closer to the targeted vectors $\{t_1, t_2, t_3, \dots, t_Q\}$. Then, output o_k from neurone k , which relates to the input neurone j through interconnection weight w_{ij} and the bias b , is obtained by

$$o_k = f\left(\sum_i^Q w_{ik}o_i + b\right) \tag{9}$$

where $f(x)$ is a transfer or sigmoid function used. The two most used transfer functions in a neural network are the logistic function and hyperbolic function respectively given by (Deo et al. 2001).

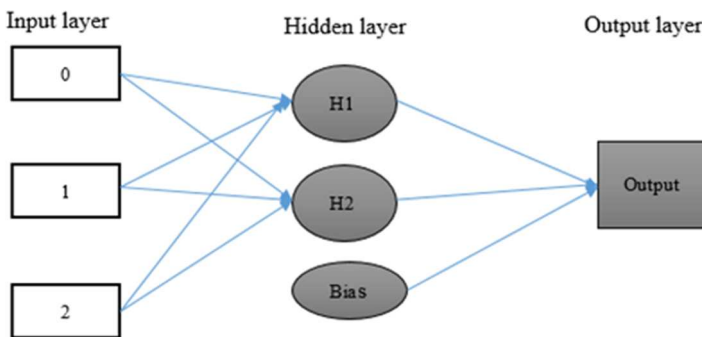


Figure 1. Multi-layer perceptron model.

Logistic Function

$$f(x) = \frac{1}{1 + \exp(-x)} \quad (10)$$

Hyperbolic HTangent Function

$$f(x) = \frac{1 - \exp(-x)}{1 + \exp(-x)} \quad (11)$$

Letting the target state of the output neurone be t , then an error (e) at the output neurone k is defined as

$$e = \frac{1}{2}(t_k - o_k)^2 \quad (12)$$

In training a network, the difference between the output and the targeted values are compared and adjustments are made to the weights and bias to reduce the error function given in Equation (12). This process can also be labelled as the learning process of a network. Weights and biases are readjusted so that the error function becomes minimal making a network converge more closely to a targeted value.

Training a network is known to be the final stage of developing a model. There are no fixed techniques for determining the exact number of nodes and layers in a network formed. Model parameters are varied and the one that yields the desired error is preferred. The main objective of any training algorithm is to minimise the error function. The error function is defined as

$$E = \frac{1}{P} \sum_{p=1}^P E_p \quad (13)$$

where P is the total number of training patterns and E_p is the error for the training pattern defined by

$$E_p = \frac{1}{2} \sum_{k=0}^N (t_k - o_k)^2 \quad (14)$$

where N is the number of training values, o_k is the output, and t_k is the target output. Error function (E) is minimised by making small adjustments to the weights and the bias functions till a strong map between the predicted and actual value is achieved in the training process (Li et al. 2009). One of the most common training algorithms widely used in forecasting is the error backpropagation algorithm. This technique is often referred to as an error-correction rule because it systematically reduces the error by adjusting the network's weights. The error backpropagation algorithm comprises two phases. In the forward phase, the input vectors are passed through a series of hidden layers where small weights together with a bias are attached and are finally passed through a sigmoid function to reach a target. In this process, weights and biases remain fixed. In the backward phase, weights and bias values are readjusted to acquire a minimal error function. Once the error value is obtained, it is re-directed through the network for more adjustment to the weights and biases to converge more

closely to the required output. This is usually achieved by the steepest descent or gradient descent approach. The weights and bias terms are modified by moving a small step in the direction of the negative gradient of the error function during each iteration. The number of iterations is repeated until a specified convergence is reached which gives a very small coefficient correlation (Deo et al. 2001). The gradient descent is given by (Deo et al. 2001).

$$X_{k+1}^- = X_k^- - ng^- \quad (15)$$

Where X^- is the vector of weights at $k + 1$ iterations, X_k^- is the vector of weights at k th iteration n is the step size and g^- is the gradient vector $= \nabla f(X^-)$, where $\nabla f(X^-)$ is the error function for a weight vector X^- . After this process, model parameters are kept fixed and used on the testing data for validation before the model is considered optimum for forecasting.

Methodology

This section elaborates on the variables used while developing different forecasting models, namely, time series models, regression models, and ANN models, to forecast the wave energy generated at near-shore areas in the Fiji Islands.

Data and variables

The variables used in this research are the *wave height*, *wave period*, and the *wave power* (precisely, the wave power transmitted per unit width of crest). Wave height and wave period are the independent variables while power is the dependent variable. In model development, ‘lags’ refer to the use of past values of a variable as predictors for its future values. If there are irregular intervals in the data, then defining and using these past values consistently becomes challenging, hence the number of such historical points (lags) that can be effectively incorporated into the model will be limited. The data collated in this study did not have a fixed frequency resulting in irregular intervals, hence the lags for each independent variable will be limited while developing the models.

The data for this research was collected by the University of the South Pacific’s researchers. Data was collected near Tagaqa, Sigatoka in Fiji from 10th October 2009 to 13th December 2010. A Valeport Midas Directional Wave Recorder (DWR) was employed for the measurements. The DWR is provided with a high-accuracy piezo-electric pressure sensor for water height measurements. Moreover, the DWR contains a flux gate compass and a Valeport two-axis Electromagnetic current sensor. A PRT-type temperature sensor was also active and recorded temperature readings at the location. A sampling frequency of 1 Hz was chosen to sample data for 1024 s. This frequency ensures that waves of up to 0.3 Hz (3.33 s) are accurately recorded. Since waves caused by meteorological events lie in the period range of 7–15 s, this sampling frequency ensured optimal use of memory and batteries for long-term deployment. From the raw data, the significant wave height, period and mean direction were extracted. The DWR requires 32 D-sized batteries that are replaced every month (Ram et al. 2014). Approximately 3039 data values were gathered (244 days @ 2-hour data = 2928 data values, 111 days @ daily data = 111 data values). Further details on the data collection and selection

can be found in the paper by Ram et al. (2014). From this, only 2860 data values are used while developing different forecasting models. The 2860 data values were in the form of wave height, wave period, and wave direction. This data was recorded at every two-hour interval throughout the duration. The first 80% of the data was used to train the models while the remaining 20% of data was used for the testing and validation process.

Pre-processing of data is done before the training process of model development. Mathematical models require processed or normalised data so that they can generalise and learn the relevant patterns to minimise the error function (Kimata 2016). In addition, if data is not normalised to an appropriate range, then the network will not converge during the training process providing less meaningful output.

Data can be normalised to a range of [0,1] as discussed by Kumar et al. (2020) by Equations (16) and (17):

$$x_n = \frac{x_o - x_{\min}}{x_{\max} - x_{\min}} \quad (16)$$

where x_n is the pre-processed data, x_o is the actual data value, while x_{\min} and x_{\max} are the maximum and minimum values of the data.

The normalised data to be in the range of $[-1, 1]$ could be obtained by

$$x_n = SR_{\min} + SF(x - x_{\min}) \quad (17)$$

where $SF = (SR_{\max} - SR_{\min}) / (x_{\max} - x_{\min})$ is the scale factor, x is the actual value, SR_{\min} and SR_{\max} are upper and lower scaling range limits, and x_n is the pre-processed value.

Generally, a single hidden layer network has a form ANN(a,b,c) indicating the model has a number of input nodes, b number of nodes in the hidden layer, and c number of nodes in the output layer. Similarly, a two-hidden-layer ANN model has a form ANN(d,e,f,g) where it has d number of input nodes, e number of nodes in the first hidden layer, the f -number of nodes in the second hidden layer with g number of nodes in the output layer. The most extensively used ANN model for many forecasting problems is the backpropagation neural network. It is a multi-layer feedforward neural network with error backpropagation for a model to converge to the output value by introducing and adjusting the weights.

The *R* software is used to develop the backpropagation neural network using the training data for forecasting wave power. The network consists of two arcs with the first arc connecting the input nodes to the hidden nodes and the second arc connecting the hidden nodes to the output nodes. The input layer has two nodes, which are the wave height and the wave period. In this research, several ANN models were developed while trying to identify the model parameters and achieve the optimum ANN model.

ANN and regression models were developed using *R* software version 3.6.2 which requires the developer to write the codes while developing, training and testing the models formed despite having different inbuilt libraries. The optimum ANN model was obtained by minimising the Sum of Squared Error (SSE) while an optimum regression model was obtained by using the least square error method. Once the optimum model was identified, the coefficients were kept fixed during the testing phase of the models.

EView 8.0, a statistical software, was used to develop time series models such as single exponential smoothing, trend-adjusted double exponential smoothing, HW additive, HW multiplicative, and ARIMA models. EView software was further used to generate

and display model parameters and the graphs of actual, fitted, and residuals. The benchmark model (naïve model) was developed using Microsoft Excel 2016 version. The performance of all the models developed is then compared to this benchmark model and the results are presented in Section ‘Results’ of the paper.

Model performance indicators like the Mean Squared Error (MSE), Root Mean Squared Error (RMSE), Mean Absolute Error (MAE), Mean Absolute Percentage Error (MAPE), and correlation coefficient or goodness-of-fit (R^2), as presented in Table 1, were estimated using the R software together with graphs of actual, fitted, and residuals for each of these models. The best forecasting model was identified based on their performance against these model evaluators. The optimum model is the one with the lowest values of MAE, MAPE, MSE, RMSE, and SSE and with the highest R^2 value.

The wave power (P), which is actually the mean power transmitted per unit width of crest, can be found using Equation (18)

$$P = \frac{1}{8} \rho g H^2 c_g \tag{18}$$

where ρ = water density, g = gravity, H = wave height, and c_g , the group velocity, is defined for any finite depth of water (depth = h) as:

$$c_g = \frac{1}{2} \left[1 + \frac{2kh}{\sinh 2kh} \right] \frac{gT}{2\pi} \tanh(kh) \tag{19}$$

where k = wave number, h is the mean water depth and T = wave period. These equations are obtained from the linear wave theory which is developed with certain assumptions. The present measurements were performed at a location 668 m from the shoreline. The waves are mostly uni-directional coming from the South-west direction (the waves normally lose their multi-directional nature as they approach the shoreline). The wavelength, estimated for the depth at the location, reduced by about 40% compared to the deepwater wavelength and the measured mean significant wave height was 1.23 m. A spectral analysis was performed by applying a fast Fourier transform (FFT). With the frequency analysis and the mean pressure, the wave data were passed through the reverse Fourier transform to back calculate the surface elevation for every

Table 1. Model evaluators used in this study.

Sum of Squared Error or Residual (SSE)	$= \sum e_t^2 = \sum (Y_t - A_t)^2$
Mean squared Error (MSE)	$= \frac{1}{n} \sum e_t^2 = \frac{1}{n} \sum (Y_t - A_t)^2$
Mean Absolute Error (MAE)	$= \frac{\sum (Y_t - A_t) }{n}$
Mean Absolute Percentage Error (MAPE)	$= \frac{100}{n} \left(\sum \left(\frac{ A_t - Y_t }{A_t} \right) \right)$
Root Mean Squared Error (RMSE)	$= \sqrt{\frac{\sum (Y_t - A_t)^2}{n}}$
Goodness-of-fit: R^2	$= 1 - \frac{\sum (Y_t - A_t)^2}{\sum (Y_t - \bar{A})^2}$

where Y_t is the forecasted value, A_t is the observed value, n is the number of observations, and \bar{A} is the mean of the observed values.

sample in the burst. The frequency spectra from the DWR data were obtained which defines the sea state in each burst. From the spectrum, the wave height and period were estimated (Ram et al. 2014). Based on these characteristics, the above equations can be used to estimate the wave power with reasonable accuracy as the linear wave theory is grossly violated (Holthuijsen 2010).

Results

In this section, the results for the time series model, the regression model, and the ANN model are presented. EView statistical software was used to develop the time series models. The results obtained using EView for each model using training and testing samples are displayed in the table below. The smoothing coefficient α was fixed while using the test data.

Exponential smoothing method

Forecasting wave energy is carried out using exponential smoothing methods. The results for the single exponential smoothing method are presented in Table 2 for training and testing data, respectively.

The value of α ($= 0.696$) is close to 1 which indicates that the estimate favours more recent data than the distant observations.

Table 3 presents the results of the double exponential smoothing method. It is observed that the value of $\alpha < 0.5$, this means that the estimation favours past distance observation in contrast to single smoothing.

The results from Table 2 show that the single exponential smoothing model had a sum of squared residual value of 16787.02 and root mean squared error value of 5.3161, while the double exponential smoothing model had a sum of squared residual value of 19537.00 and root mean squared error value of 5.7350, both of which are much higher than those of the single exponential smoothing model. These results from both the training and testing data show that the single exponential smoothing model performed well compared to the double exponential smoothing model.

Holt-Winter (HW) additive & multiplicative method

HW method of forecasting is an extension of the exponential smoothing method (Tirkes et al. 2017). This technique best works when the data series exhibits a linear trend with seasonality which most of the models fail to capture while forecasting. Tables 4 and 5 display the results from EView using the training and testing data, respectively, for additive and multiplicative models. While testing, the parameter values were kept fixed.

Table 2. Results of single exponential smoothing model using training and testing data.

	Training Data ($n = 2267$)	Testing Data ($n = 594$)
Parameter, α	0.6960	0.6960
Error Values		
Sum of Squared Residual	64611.91	16787.02
Root Mean Squared Error	5.3386	5.3161

Table 3. Results of double exponential smoothing model using training and testing data.

	Training Data (n = 2267)	Testing Data (n = 594)
Parameter, alpha (α)	0.3420	0.3420
Error Values		
Sum of Squared Residual	74043.66	19537.00
Root Mean Squared Error	5.7150	5.7350

Table 4. Results of HW additive method using training and testing data.

	Training Data (n = 2267)	Testing Data (n = 594)
Parameters, alpha (α)	0.7000	0.7000
beta (β)	0.0000	0.0000
gamma (γ)	0.0000	0.0000
Error Values		
Sum of Squared Residual	64296.52	16499.95
Root Mean Squared Error	5.3256	5.2705

For the HW additive and multiplicative models, the coefficients $\beta = \gamma = 0$ indicate that the model favours past data for the input variables compared to the present data. However, $\alpha > 0.5$ indicates that the model is more persistent to present data for the mean component of the model. The coefficient of trend using training data is positive which implies that there is a general improvement in the model as more present data are used. The seasonal effect which has a very small range indicates that the seasonal component has a limited influence on the forecasted values.

Forecasting using the arima technique

An ARIMA model has a form of ARIMA(p,d,q) where p is the autoregressive term, d is the differencing used while attaining stationarity of data while q is the moving average term in a model. The ARIMA model is defined by:

$$y_t = \sum_{i=1}^P \varphi_i y_{t-i} + \sum_{j=1}^q \theta_j e_{t-j} + \varepsilon_t,$$

where φ_i is the i th autoregressive parameter, θ_j is the j th moving average parameter and ε_t is the error term at time t .

Before an ARIMA model can be developed for forecasting wave energy, the stationarity of the data is investigated by interpreting a time series plot shown in Figure 2, which clearly shows that the training data fluctuates around the mean of 11 kW/m. The wave power presented in Figure 2 was calculated using Equation (18) from the measured

Table 5. Results of HW multiplicative method using training and testing data.

	Training Data (n = 2267)	Testing Data (n = 594)
Parameters, alpha (α)	0.7000	0.7000
beta (β)	0.0000	0.0000
gamma (γ)	0.0300	0.0000
Error Values		
Sum of Squared Residual	64434.28	16426.75
Root Mean Squared Error	5.3313	5.2588

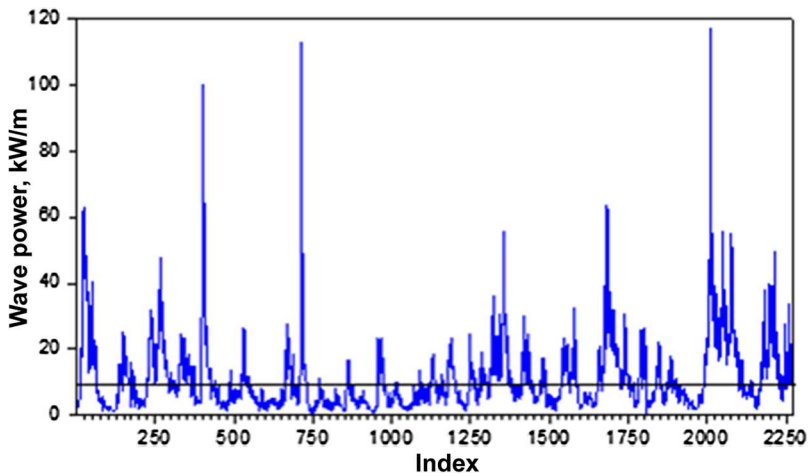


Figure 2. Time series plot for actual power using training data.

wave parameters (actual wave power). The index identifies the values of the datasets. One thousand means 1000 values and 1 means the first value of the dataset.

The stationarity of input data is further checked by conducting a unit root test using the Augmented Dickey-Fuller (ADF) test ($t = -8.8703$, p -value < 0.0001), which indicates that the wave energy data is stationary (please see [Table A1](#) in Appendix A). Apart from the time series plot and unit root test, the stationarity of input data is further verified by the Autocorrelation Factor (ACF) using the correlogram as shown in [Table A7](#) in Appendix A. It shows that ACF drops to 0 quickly in an exponential decay during a short period, which again clearly supports the above results. This means that no differencing is required thus the d term in the ARIMA model will be 0.

Further, after closely studying the values of ACF and Partial Autocorrelation Factor (PACF) from [Table A7](#), it is evident that the model will have both an autoregressive and moving average term. Since the spikes are observed at lags 1, 2, and 3 in the PACF graph, the p and q values can be considered as 1, 2, and 3 only.

Results of ARIMA model selection using the training data

Model parameters p and q are varied, and the performance of each combination is measured against the model selection measures which are Akaike's Information Criterion (AIC), the Schwarz's Bayesian Information (BIC), the Sum of Squared Error (SSE), and the adjusted R^2 values. The lowest values of the measures AIC, BIC, SSE and the highest value of adjusted R^2 identify the better model. [Table 6](#) presents some results of ARIMA models used to fit the training data with different model parameters (with the best values of the measures in bold).

The results show that ARIMA (1,0,1) model performed the best as it recorded the lowest values of AIC, BIC, and SSE with the highest value of adjusted R^2 . The results of ARIMA (1,0,1) obtained from the EViews are presented in [Table 7](#).

Finally, the performance of different time series models developed is compared using the model evaluators discussed in the methodology. [Table 8](#) compares the performance parameters of each time series model to identify the optimum time series model for forecasting.

Table 6. Model selection criteria of ARIMA training model.

Model	AIC	BIC	SSE	Adjusted R^2
ARIMA (1,0,0)	6.203337	6.208391	65477.79	0.765874
ARIMA (3,0,0)	6.793679	6.798736	118057.1	0.577818
ARIMA (0,0,1)	6.974139	6.979191	141592.8	0.49386
ARIMA (0,0,2)	7.082566	7.087618	157808.5	0.435895
ARIMA (1,0,1)	6.157499	6.16508	62488.99	0.776462
ARIMA (1,0,3)	6.203821	6.211401	654451.7	0.765864
ARIMA (2,0,1)	6.190849	6.198433	64579.57	0.768918
ARIMA (2,0,3)	6.570971	6.578554	94445.21	0.662051
ARIMA (3,0,1)	6.570126	6.577712	94323.69	0.662393
ARIMA (3,0,3)	6.782727	6.790313	116668.1	0.582417

Table 7. Results of ARIMA (1,0,1) using training data.

Variable	Coefficient	Std. Error	t-Statistic	Probability
C	11.38192	1.205429	9.442214	0.0000
AR(1)	0.931765	0.008592	108.4422	0.0000
MA(1)	-0.255051	0.022918	-11.12891	0.0000
R-squared	0.776660	Mean dependent variable		11.2822
Adjusted R-squared	0.776462	S.D. dependent variable		11.1144
S.E. of regression	5.254840	Akaike info criterion		6.1575
Sum squared resid	62488.99	Schwarz criterion		6.1651
Log likelihood	-6973.446	Hannan-Quinn criterion		6.1603
F-statistic	3934.761	Durbin-Watson statistic		1.9867
Prob(F-statistic)	0.000000			

Table 8. Comparison of time series models based on training data set.

Model	SSE	MSE	RMSE	MAPE	MAE	R^2
Single Exponential	64611.91	28.5011	5.3386	56.80	2.884	0.7691
Double Exponential	74043.66	32.6615	5.7150	56.67	3.042	0.7354
HW Additive	64296.52	28.3619	5.3256	57.48	2.896	0.7707
HW Multiplicative	64434.28	28.4227	5.3313	55.52	2.886	0.7698
ARIMA (1,0,1)	62647.7	27.622	5.2580	59.167	2.9078	0.7767

The table shows that ARIMA (1,0,1) model performed the best, recording the highest R^2 value and the lowest value of SSE, MSE, and RMSE (bold numbers). The other time series models performed relatively close to the optimum time series model. The results of ARIMA(1,0,1) using testing data will be discussed in the discussion section.

Figure 3 displays the graph of actual vs. predicted wave power using the testing data using ARIMA(1,0,1) model. The wave power presented in Figure 3 was also calculated using Equation (18). It can be seen that the predicted wave power was generally higher than the actual wave power for most of the index values; between index values of 250 and 340, it consistently overpredicted the wave power. Similarly, after the index values of 520, there was consistent overprediction using the ARIMA (1,0,1) model.

Forecasting power generation using regression models

The relationship between the wave power, wave height and wave period are investigated through the correlation coefficient and through the contour plot analysis as shown in Table 9 and Figure 4 respectively.

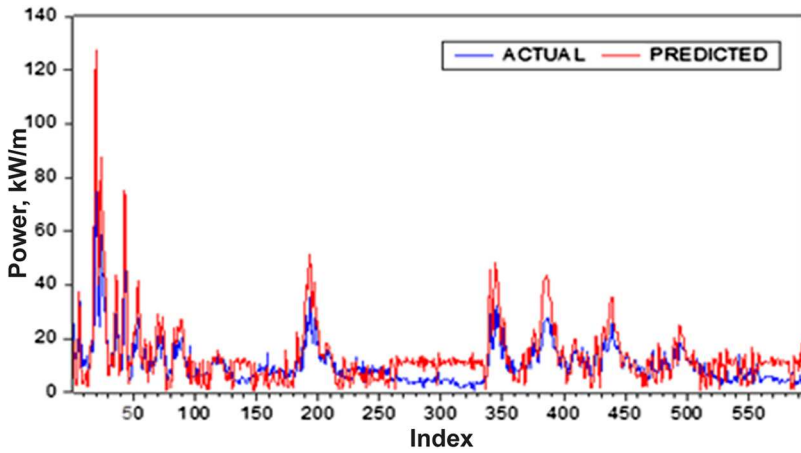


Figure 3. Actual vs. predicted wave power with ARIMA (1,0,1) model using testing data.

Table 9. Correlation between input and output variables.

	Wave Height	Wave Period	Wave Power
Wave Height	1.0000	0.0947	0.9253
Wave Period	0.0947	1.0000	0.3456
Wave Power	0.9253	0.3456	1.0000

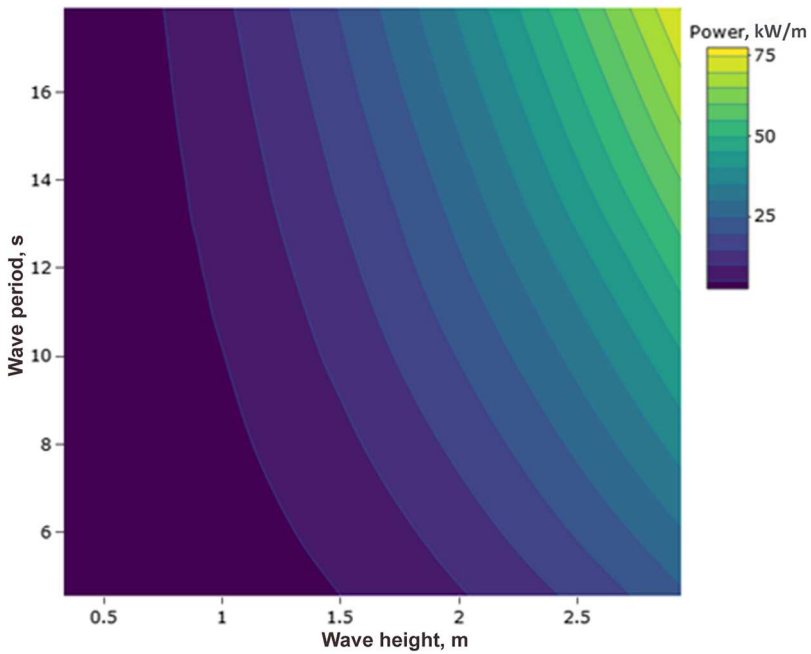


Figure 4. Contour plot of fitted and continuous variables.

Wave height and power show a strong correlation with a coefficient of 0.9253. The wave period and wave power have a small correlation coefficient of 0.3456. The two input variables of wave height and wave period show an extremely low correlation with each other with a correlation coefficient of 0.0947, which clearly shows less multi-collinearity effect in the regression model. Thus, both the input variables were selected to develop the regression models.

Contour plot analysis

The relationship between the variables is further investigated by studying the contour plot. The independent variables are placed on the X and Y axis while the response variable is represented by coloured contours which are given by the Z value.

Using the `plot_ly` function in 'plotly' package in the R software, the contour plot, shown in Figure 4, was generated to visualise the wave power at different wave heights and wave periods.

The contour plot suggests that the wave height has a stronger influence on the amount of wave power compared to the wave period. Wave period alone does not have much significant impact on the wave power as increasing only the wave period by 2 s accounts for the power increase of roughly about 2 kW/m. However, increasing the wave height by 0.5 m results in a wave power of roughly 23 kW/m. It can also be noted that the maximum wave power can be generated by having a wave height of more than 2.5 m with a wave period set at more than 15 s. The plot also suggests that the wave power shows a non-linear relationship with smaller values of wave height and wave period. The contour plot further highlights that when the values of independent variables increase, the relationship shows a predictable pattern.

Equations (18) and (19) suggest that wave power has a nonlinear relationship with its independent variables, wave height and wave number. It can be seen that with increasing wave height, the wave power increases considerably. At lower wave heights, the power did not increase much even at high wave periods; however, increasing the wave height at higher wave periods shows a dramatic increase in the power.

Linear regression models

This section presents the different Linear Regression Models (LRM) developed as discussed below for forecasting power energy for training data using R software:

LRM 1: Linear regression model with wave height as the input variable, that is:

$$\text{Power} = \beta_0 + \beta_1 \cdot \text{wave height} + \varepsilon$$

LRM 2: Linear regression model with wave period as the input variable, that is:

$$\text{Power} = \beta_0 + \beta_1 \cdot \text{wave period} + \varepsilon$$

LRM 3: Linear regression model with two input variables wave period and wave height, that is:

$$\text{Power} = \beta_0 + \beta_1 \cdot \text{wave period} + \beta_2 \cdot \text{wave height} + \varepsilon$$

LRM 4: Linear transformation of a polynomial regression model which is the quadratic form of wave height that influences the wave power as given below:

$$\text{Power} = \beta_0 + \beta_1 \cdot \text{wave height} + \beta_2 \cdot (\text{wave height})^2 + \varepsilon$$

LRM 5: A Box–Cox transformation model. From the results presented in Appendix A and Tables A2–A5 for the LRM models 1–4, it can be seen that the model LRM 3 was found to be the best linear regression model based on the model selection criteria with the highest R^2 value and the smallest AIC, BIC, Bias, SSE, and the root mean square error of the residuals (S_p). Thus, using the LRM 3 the optimum value of parameter lambda (λ) to construct the Box–Cox transformation model is obtained as $\lambda = 0.5$, which gives the corresponding nonlinear regression model as a square root of wave power, that is:

$$\sqrt{\text{Power}} = \text{wave period} + \text{wave height} + \varepsilon$$

or

$$\text{Power} = (\text{wave period} + \text{wave height})^2 + \varepsilon$$

which gives the Box–Cox linear transformation model as of the form:

$$\begin{aligned} \text{Power} = & \beta_0 + \beta_1 (\text{wave period})^2 + \beta_2 (\text{wave height})^2 \\ & + \beta_3 (\text{wave period}) \cdot (\text{wave height}) + \varepsilon \end{aligned}$$

The results of the regression coefficients for all five models developed using the training data are presented in Tables A2–A6 in Appendix A and the performance of models is measured against different selection criteria (AIC, BIC, SSE, bias, S_p and R^2 with the best values in bold) and presented in Table 10.

The model LRM5, which was developed using the Box–Cox transformation, performed the best when compared to other regression models as it recorded the lowest value of AIC, BIC, SSE, S_p , and the highest adjusted R^2 value. Figure 5 displays the actual and predicted values of the power for LRM5 using the training data set.

Further, Figure 6 displays the graph of actual vs. predicted power using the model LRM5 with the testing data. The model parameters obtained for training data were kept fixed while running them through the testing data.

However, before LRM5 is considered as the optimum regression model, it is imperative to study its residual analysis. Conducting the residual analysis and the diagnostic tests for the models, the results presented in Appendix B, namely Figures B1–B3, suggest that these regression models failed to meet the criteria for linearity, independence, and normality tests, which means the linear regression models' goodness of fit test may not be a powerful measure to consider, thus, limiting to detect the best linear fit model.

Table 10. Performance of regression models developed using the training data.

Model	AIC	BIC	SSE	Bias ($\times 10^{-14}$)	S_p	Adjusted R^2
LRM1	11467.32	11484.36	25391.52	1.538	3.429	0.8570
LRM2	15385.32	15402.36	155497.00	7.690	8.485	0.1245
LRM3	10160.80	10183.51	13862.37	5.489	2.534	0.9219
LRM4	10537.62	10560.33	16501.81	-0.109	2.765	0.9071
LRM5	8679.30	8707.69	6979.72	0.221	1.798	0.9607

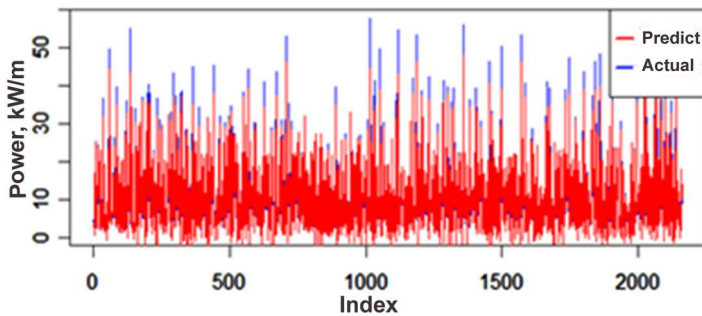


Figure 5. Actual vs. predicted power for LRM5 using the training data.

Forecasting wave power using artificial neural network

Tables C1 and C2 in Appendix C display the results of some of the ANN models developed using the training data set with logistic and tangent hyperbolic activation functions while varying the model parameters. Based on the results presented in Table C1, ANN (2,4,2,1) performs best when compared with other models developed using the logistic transfer function given in Equation (10). The performances of the models beyond ANN (2,5,1) and ANN (2,4,3,1) are not documented since they did not show significant improvement. A 3-hidden layer network is also investigated and its performance is compared against single and two hidden layer networks. The 3-hidden layer networks did not perform well against the two hidden layer networks hence it was not investigated beyond ANN (2,3,3,3,1).

Similarly, based on the results presented in Table C2, ANN (2,7,2,1) is the best model when using the tangent hyperbolic transfer function (Tanh) given in Equation (11). ANN (2,7,2,1) is a 2-hidden layer network with two nodes in the input layer, seven nodes in the first hidden layer, two nodes in the second hidden layer, and a single node in the output layer. The performances of models beyond ANN (2,8,1) and ANN (2,7,3,1) were not documented as they did not show significant improvement in terms of the error values.

After a close comparison between the performances of two transfer functions, model ANN (2,7,2,1) developed using tangent hyperbolic function performed best, recording the lowest MSE, MAE, MAPE, and RMSE values and the highest R^2 value as shown in

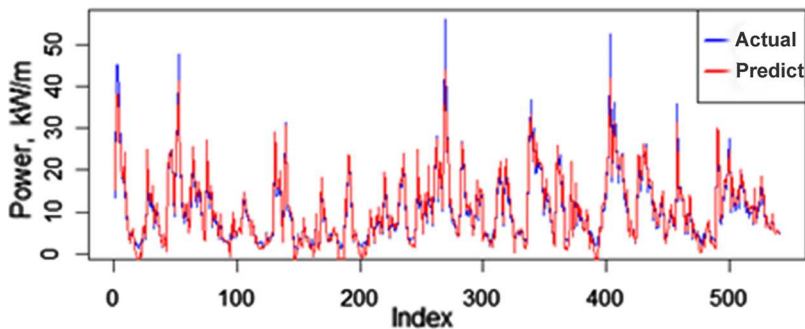


Figure 6. Actual vs. Predicted power for the best regression model- LRM5.

Table 11. Comparison of optimum ANN model formed using the two-transfer function.

Transfer Function	ANN Model	MSE	MAE	RMSE	MAPE	R ²
Logistic	ANN(2,4,2,1)	0.0897	0.1476	0.2995	2.6741	0.9989
Tangent	ANN(2,7,2,1)	0.0076	0.0655	0.0874	1.2663	0.9999

Table 11. Therefore, it is found that ANN (2,7,2,1) is the best ANN model, with the better performance measures in bold, used to forecast the wave power.

The R software was further used to generate the structure of the optimum ANN model, ANN(2,7,2,1). Figure 7 displays the architecture of model ANN(2,7,2,1).

ANN (2,7,2,1) was further used on the testing data and its performance parameters (with the best values in bold) based on different model evaluators is presented in Table 12. Weights and bias terms for ANN (2,7,2,1) model were fixed while running through the testing data. The graphs of actual vs. the predicted power are discussed in Section ‘Discussion’ together with the residual plot for the proposed ANN (2,7,2,1) model.

Discussion

The results in the previous section reveal that the best time series model was ARIMA (1,0,1), the best regression model was LRM5 which was a Box–Cox transformation model and the best ANN model was ANN (2,7,2,1) with a tangent hyperbolic transfer function. The performance of these models is analysed by comparing the R² and different error measures as presented in Table 12.

From the results presented in Table 12, the ANN (2,7,2,1) model which was the proposed model, produced the highest R² value which is the optimal out of the three models.

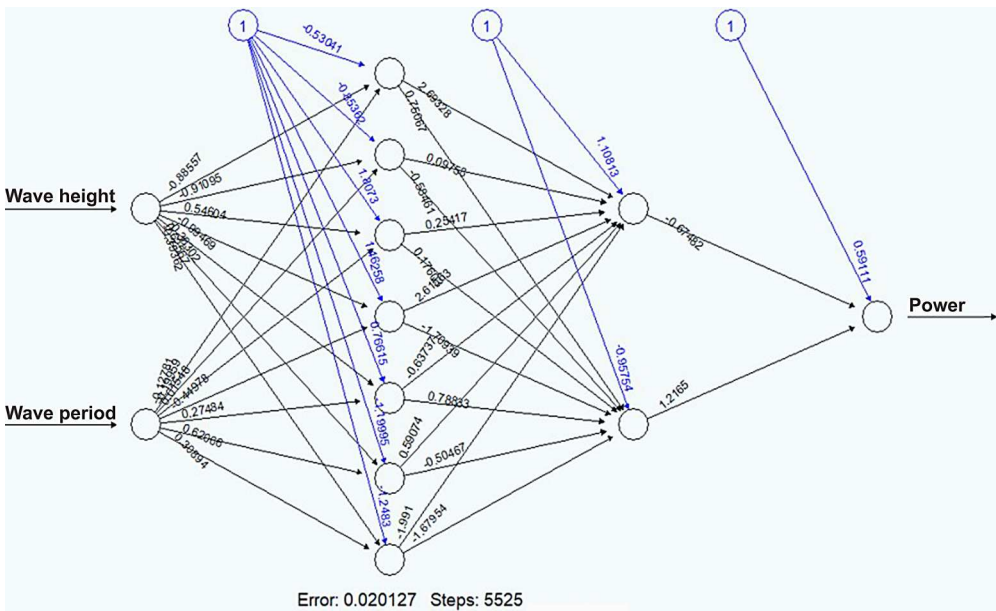


Figure 7. Architecture for proposed ANN (2,7,2,1) model with tangent hyperbolic transfer function.

Table 12. Performances of optimum model formed using the training dataset.

Model	MSE	RMSE	MAPE	MAE	R^2
ARIMA (1,0,1)	27.6220	5.2580	59.1670	2.9078	0.7765
LRM5	3.2284	1.7968	23.4369	2.6100	0.9607
ANN (2,7,2,1)	0.0076	0.0874	1.2663	0.0655	0.9999

Table 13. Results of identified optimum models using the testing dataset.

Model	MSE	MAE	RMSE	MAPE	R^2
ARIMA (1,0,1)	27.9340	5.6429	7.8083	80.7457	0.5657
LRM5	2.7001	0.1707	1.6434	20.1357	0.9591
ANN (2,7,2,1)	0.1650	0.3106	0.4061	4.9059	0.9975

When the other measures are compared, it is again seen that the ANN (2,7,2,1) model produced the lowest values for the MSE, RMSE, MAPE and MAE which is a confirmation of its best results. Thus, we see that the proposed ANN (2,7,2,1) model outclassed all other models when tested using the training data.

Moreover, the model parameters were kept fixed and were used on the testing data and the performance based on the model evaluators is displayed in Table 13 with the best evaluators highlighted in bold.

ANN (2,7,2,1) model performed the best when compared to other models using the testing data as well. It recorded the highest R^2 value, lowest MSE, RMSE, MAPE, and second lowest MAE values. Figures 8 and 9 display the graphs of actual vs. predicted power and the residual for the optimum model developed using testing data for the ANN (2,7,2,1) model. It can be seen that the predicted power very closely matches the actual power (obtained from the measured wave height and wave period). The residual plot indicates a small variation on both sides with three outliers, indicating the acceptable accuracy of the ANN model. Comparing this to the predicted power using ARIMA (1,0,1) model, it can be seen that the ARIMA (1,0,1) model overpredicted the higher power values and underpredicted the lower power values (shown in Figure 3). On the other hand, the LRM5 model underpredicted most of the power values (Figure 6) although for both the models, the error estimates showed good accuracy. The overprediction and underprediction of the time series and regression models will not help in good control system design and hence the performance of the wave energy converter.

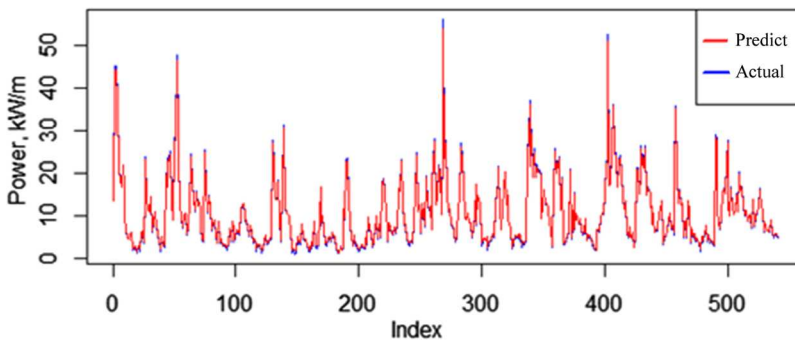


Figure 8. Actual vs. predicted wave power for ANN (2,7,2,1) model.

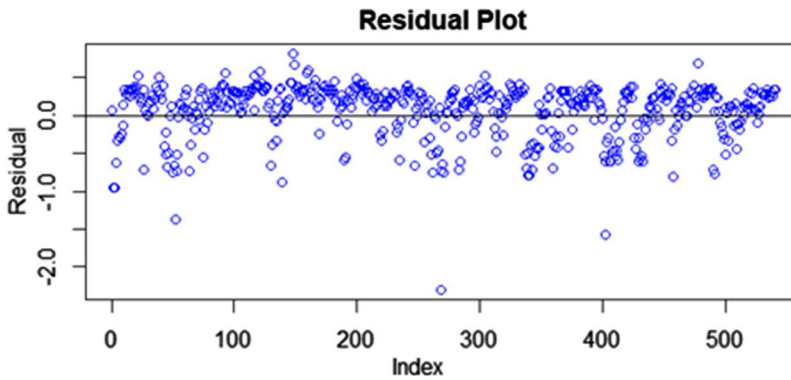


Figure 9. Residual plot for ANN (2,7,2,1) model.

Table 14. Comparison of the naïve model against the proposed model using the training dataset.

Model	MSE	RMSE	MAPE	MAE	R^2
ANN (2,7,2,1)	0.0076	0.0873	1.2664	0.0654	0.9999
Naïve model	24.14478	4.9008	35.8370	2.8402	0.7664

Table 15. Comparison of the naïve model against the proposed model using the test dataset.

Model	MSE	MAE	RMSE	MAPE	R^2
ANN (2,7,2,1)	0.1650	0.3106	0.4061	4.9059	0.9975
Naïve model	13.961	2.6296	3.7333	29.166	0.5705

The proposed ANN (2,7,2,1) model was further compared with the benchmark model; the naïve forecasting model and the results are presented in Tables 14 and 15. The naïve forecasting model is created using Microsoft Excel as stated in Section ‘Naïve method of forecasting’. The naïve model is considered the benchmark in the area of modelling and the results are presented in Tables 14 and 15 with the better performance parameters highlighted in bold.

The proposed ANN (2,7,2,1) model performed best when compared to the naïve model using both training and testing data. It recorded the highest R^2 and the lowest values for MSE, MAE, RMSE, and MAPE using both training and testing datasets. The empirical results reveal that the proposed ANN (2,7,2,1) model is more efficient and accurate in forecasting wave energy in comparison to the regression and time series models.

The contour plot presented in Figure 4 clearly shows that the wave power depends strongly on the wave height. A significant increase in wave power can be seen when the wave height is increased from 1 m to 2.5 m. The wave period started showing strong influence only at greater wave heights; at the periods of 14 s and higher, the power increased dramatically. The results reported by Ram et al. (2014) and Reddy and Ahmed (2014) both had similar wave periods. The wave periods in this range are predominantly wind/gravity waves. Waves of such characteristics are predictable and it will be much easier to design simple and robust controllers for wave energy converters. By incorporating impedance matching, maximum power absorption and transfer can be achieved.

Conclusion

Forecasting energy using suitable techniques is extremely important for developing countries like Fiji and other Pacific Island countries. Energy and its sources need to be as reliable as possible to ensure sustainable energy production. While wave energy has shown significant prospects in bringing diversification to the current sources of energy, detailed work on its reliability needs to be investigated using a forecasting model. In this work, time series models, regressions models, and ANN models are developed to forecast the wave power generated at a site in the Fiji Islands. The results indicate that these models may be promising for forecasting wave energy; however, their robustness vastly depends on their unique properties and characteristics. The proposed ANN (2,7,2,1) model clearly outperformed the time series and regression models. The ANN model is further benchmarked against the Naïve forecasting model.

For future work, it would be interesting to capture the influence of different lags in the data so that ANN can be generally accepted as the best forecasting model for wave power. This research used the measured wave height and wave period. Different models were developed to predict the wave power and it was compared with the actual wave power. It would be interesting to investigate the performance of this model if wave height and wave period are measured in deeper waters much before the wave train reaches the shore where the power can be extracted. The success of this process can provide alternatives while discussing energy sources for the future. The present work can also be expanded to other PICs as a prospective form of energy source considering its smaller impact on the environment.

Disclosure statement

No potential conflict of interest was reported by the authors.

Funding

The work was supported by the internal funding of the University of the South Pacific to Avikesh Kumar.

Data availability statement

Sample data, both measured (actual) and predicted using ANN, are available at the repository <http://repository.usp.ac.fj/id/eprint/14442>. Additional data will be made available upon request.

ORCID

M. Rafiuddin Ahmed  <http://orcid.org/0000-0002-3514-1327>

References

Ali M, Prasad R, Xiang Y, Deo R. 2020. Near real-time significant wave height forecasting with hybridized multiple linear regression algorithms. *Renewable and Sustainable Energy Reviews*. 132:110003. doi:10.1016/j.rser.2020.110003.

- Al Khatib A. 2011. Developing a wind speed prediction tool using artificial neural networks and designing wind park in Syria using WASP software. Kassel university.
- Arzu A. 2017. Forecasting wind speed of Suva (Fiji) and Abaiang (Kiribati) using artificial neural network [MSc Thesis]. The University of the South Pacific, Suva, Fiji.
- Asma S, Sezer A, Ozdemir O. 2012. Mlr and ANN models of significant wave height on the west coast of India. *Computers & Geosciences*. 49:231–237. doi:10.1016/j.cageo.2012.05.032.
- Bandyopadhyay G, Chattopadhyay S. 2007. Single hidden layer artificial neural network models versus multiple linear regression model in forecasting the time series of total ozone. *International Journal of Environment Science Technology*. 4(1):141–149. doi:10.1007/BF03325972.
- Barak S, Sadegh S. 2016. Forecasting energy consumption using ensemble ARIMA–ANFIS hybrid algorithm. *Electrical Power and Energy Systems*. 82:92–104. doi:10.1016/j.ijepes.2016.03.012.
- Coe RG, Bacelli G, Forbush D. 2021. A practical approach to wave energy modeling and control. *Renewable and Sustainable Energy Reviews*. 142:110791. doi:10.1016/j.rser.2021.110791.
- Contreras J, Espinola R, Nogales F, Conejo A. 2003. Arima models to predict next-day electricity prices. *IEEE Transactions on Power Systems*. 18(3):1014–1020. doi:10.1109/TPWRS.2002.804943.
- Cyprien B, Reddy SK, Kruger J.. 2015. Waves and coasts in the Pacific – cost analysis of wave energy in the Pacific. Secretariat of the Pacific Community. 1–54.
- Deo M, Jha A, Chaphekar A, Ravikant K. 2001. Neural networks for wave forecasting. *Ocean Engineering*. 28:889–898. doi:10.1016/S0029-8018(00)00027-5.
- Dumicic K, Casni A, Gogala Z. 2008. Evaluating Holt’s Double Exponential and Linear trend forecasting of basic tourism time series in Croatia. *International Conference Proceedings, Zagreb, Croatia*.
- Ensafi Y, Amin SH, Zhang G, Shah B. 2022. Time-series forecasting of seasonal items sales using machine learning – a comparative analysis. *International Journal of Information Management Data Insights*. 2(1):100058. doi:10.1016/j.jjime.2022.100058.
- Felix A, Hernandez-Fontes JV, Lithgow D, Mendoza E, Posada G, Ring M, Silva R. 2019. Wave energy in tropical regions. Deployment challenges, environment and social perspective. *Journal of Marine Science and Engineering*. 7:219. doi:10.3390/jmse7070219.
- Hadadpour S, Etemad-Shahidi A, Kamranzad B. 2014. Wave energy forecasting using artificial neural networks in Caspian Sea. *Proceedings of the Institute of Civil Engineers - Maritime Engineering*. 167:42–52. doi:10.1680/maen.13.00004.
- Hatalis K, Pradhan P, Kishore S, Blum R.. 2014. Multi-step forecasting of wave power using a non-linear recurrent neural network. In: 2014 IEEE PES General Meeting Conference and Exposition. 1–5. National Harbour, Maryland, USA: IEEE.
- Holthuijsen LH. 2010. *Waves in oceanic and coastal waters*. New York (USA): Cambridge University Press.
- Hsu CC, Chen CY. 2003. Regional load forecasting in Taiwan—applications of artificial neural networks. *Energy Conversion and Management*. 44:1941–1949. doi:https://doi.org/10.1016/S0196-8904(02)00225-X.
- IEA. 2020. *Renewables 2020 - analysis and forecast to 2025*. <https://www.iea.org/reports/renewables-2020>.
- IPCC. 2014. *Climate Change 2014: Synthesis Report. Contribution of Working Groups I, II and III to the Fifth Assessment Report of the Intergovernmental Panel on Climate Change*. <https://www.ipcc.ch/report/ar5/syr/>.
- IRENA. 2017. *Input to concept papers for Partnership Dialogues (5) and (6): Ocean Energy*. <https://sustainabledevelopment.un.org/content/documents/13416IRENA%20INPUT%20OCEAN%20CONF%20CONCEPT%20PAPERS.pdf>.
- Kalekar P. 2004. Time series forecasting using holt-winters exponential smoothing. *Kanwal Rekhi School of Information Technology*. 4329008(13):1–13.
- Kashikar VR, Mane SJ. 2014, November. Wave height forecasting using artificial neural network and fuzzy logic. *International Journal of Soft Computing and Artificial Neural Intelligence*. 2(2):33–35.

- Kavasseri R, Seetharam K. 2009. Day-ahead wind speed forecasting using f-ARIMA models. *Renewable Energy*. 34:1388–1393. doi:10.1016/j.renene.2008.09.006.
- Kimata J. 2016. Forecasting exchange rate of Solomon Islands dollar using artificial neural network and the purchasing power parity theory. Suva.
- Koehler AB, Snyder RD, Ord J. 2001. Forecasting models and prediction intervals for the multiplicative Holt–Winters method. *International Journal of Forecasting*. 17(2):269–286. doi:10.1016/S0169-2070(01)00081-4.
- Kumar A, Ahmed M, Khan M. 2020. Time-variations of wave-energy and forecasting power availability using different techniques. 22nd Australasian Fluid Mechanics Conference. Brisbane, Australia.
- Li H, Gao Q, Yang S, Ma W, Zhen D, Zhang Y. 2023. Time variation trend of wave power density in the South China Sea. *Journal of Marine Science and Engineering*. 11:608. doi:10.3390/jmse11030608.
- Li L, Wang M, Zhu F, Wang C.. 2009. Wind power forecasting based on time series and neural network. In: Proceedings of the 2009 International Symposium on Computer Science and Computational Technology (ISCSCI 2009) Huangshan, People’s Republic of China; p. 293–297.
- Makarynskyy O, Pires-Silva A, Makarynska D, Ventura-Soares C. 2002. Artificial neural networks in the forecasting of wave parameters. 7th International Workshop on Wave Hindcasting and Forecasting. Banff, Alberta, Canada. 514-522.
- Mandal S, Prabaharan N. 2010. Ocean wave prediction using numerical and neural network models. *The Open Ocean Engineering Journal*. 3:12–17. doi:10.2174/1874835X01003010012.
- OES. 2022. OES annual report: an overview of ocean energy activities in 2021. <https://www.ocean-energy-systems.org/publications/oes-annual-reports/document/oes-annual-report-2021/>.
- Osborne J. 2010. Improving your data transformations: applying Box-Cox transformations as a best practice. *Practical Assessment, Research and Evaluation*. 15:1–9.
- Ozturk S, Ozturk F. 2018. Forecasting energy consumption of Turkey by ARIMA model. *Journal of Asian Scientific Research*. 8:52–60. doi:10.18488/journal.2.2018.82.52.60.
- Palchak D. 2012. Energy management of a university campus utilizing short-term load forecasting using ANN.
- Pleños MCF. 2022. Time series forecasting using Holt-Winters exponential smoothing: application to abaca fiber data. *Problems of World Agriculture*. 22(2):17–29. DOI: 10.22630/PRS.2022.22.2.6.
- Pongdatu G, Putra Y. 2018. Seasonal time series forecasting using SARIMA and Holt-Winter’s exponential smoothing. In: Abdullah AG, Warlina L, Kurniati PS, Nandiyanto ABD, editors. IOP Conference Series. Material Science and Engineering. Vol. 407. Bandung, Indonesia: IOP; p. 012153. doi:10.1088/1757-899X/407/1/012153.
- Posterari JB, Waseda T. 2022. Wave energy in the Pacific island countries: a new integrative conceptual framework for potential challenges in harnessing wave energy. *Energies*. 15:2606. doi:10.3390/en15072606.
- Qiokata V, Khan MGM. 2015. Modelling emigration of Fiji’s population using artificial neural network. In: Ali ABMS, editor. 2nd Asia-Pacific World Congress on Computer Science and Engineering (APWC on CSE). Nadi (Fiji): IEEE; p. 1–8.
- Rajbhandari Y, Marahatta A, Ghimire B, Shrestha A, Gachhadar A, Thapa A, Chapagain K, Korba P. 2021. Impact study of temperature on the time series electricity demand of urban Nepal for short-term load forecasting. *Applied System Innovation*. 4:43. doi:10.3390/asi4030043.
- Ram K, Narayan S, Ahmed M, Nakavulevu P, Lee Y-H. 2014. In situ near-shore wave resource assessment in the Fiji islands. *Energy for Sustainable Development*. 23:170–178. doi:10.1016/j.esd.2014.09.002.
- Rao S, Mandal S. 2005. Hindcasting of storm waves using neural networks. *Ocean Engineering*. 32:667–684. doi:https://doi.org/10.1016/j.oceaneng.2004.09.003.
- Razali S, Rusiman M, Nawawi N, Arbin N. 2018. Forecasting of water consumptions expenditure using Holt- Winter’s and ARIMA. *Journal of Physics: Conference Series*. 995:012041. IOP Publishing Ltd.
- Reddy SK, Ahmed MR. 2014. In-situ wave resource assessment near Taveuni, Fiji Islands. *Journal of Renewable and Sustainable Energy*. 6:042001. doi:10.1063/1.4884636.

- Reikard G. 2013. Integrating wave energy into the power grid: simulation and forecasting. *Ocean Engineering*. 73:168–178. doi:10.1016/j.oceaneng.2013.08.005.
- Reikard G, Robertson B, Bidlot J-R. 2015. Combining wave energy with wind and solar: short-term forecasting. *Renewable Energy*. 81:442–456. doi:10.1016/j.renene.2015.03.032.
- Shen Y. 2024. Optimized systems of multi-layer perceptron predictive model for estimating pile-bearing capacity. *J. Eng. Appl. Sci.* 71:52. doi:10.1186/s44147-024-00386-x.
- Thomas J, Barve K, Dwarakish G, Ranganath LR. 2015. A review on assessment of wave energy potential. In: *National Conference on Futuristic Technology in Civil Engineering for Sustainable Development*. Bengaluru, India; p. 178–186.
- Tirkes G, Guray C, Celebi N. 2017. Demand forecasting: a comparison between the Holt-Winters, trend analysis and decomposition models. *Tehnicki Vjesnik*. 24:503–509.
- Tolesh F, Biloshchytska S. 2024. Forecasting international migration in Kazakhstan using ARIMA models. *Procedia Comput. Sci.* 231:176–183. doi:10.1016/j.procs.2023.12.190.
- Tratar LF. 2014. Improved Holt-Winters method: a case of overnight stays of tourists in republic of Slovenia. *Economic and Business Review*. 16:5–17. doi:10.15458/2335-4216.1177.
- Twidell J, Weir T. 2015. *Renewable energy resources*. London.: Routledge.
- Uyanık GK, Güler N. 2013. A study on multiple linear regression analysis. *Procedia - Social and Behavioral Sciences*. 106:234–240. doi:https://doi.org/10.1016/j.sbspro.2013.12.027.
- Vimala J, Latha G, Venkatesan R. 2014. Real time wave forecasting using artificial neural network with varying input parameter. *Indian Journal of Marine Sciences*. 43:82–87.
- Winston WL. 2003. *Operations research: applications and algorithms*. Canada: Cengage Learning; p. 1275–1317.

Appendix

Appendix A: statistical analysis for time series models.

Table A1. Augmented Dickey-Fuller test results for unit root.

Null Hypothesis: POWER has a unit root				
Exogenous: Constant				
Lag Length: 2 (Automatic-based on SIC, maxlag = 26)				
			t-Statistic	Prob.*
Augmented Dickey-Fuller test statistic			−8.870340	0.0000
Test critical values:	1% level		−3.433042	
	5% level		−2.862615	
	10% level		−2.567388	

*MacKinnon (1996) one-sided *p*-values.

Table A2. Coefficients of linear regression model 1 (LRM1).

	Estimate	Std. Error	T value	<i>p</i> -value
Intercept	−11.9972	0.2107	−56.94	<0.0001
Wave height	18.7681	0.1649	113.79	<0.0001

Table A3. Coefficients of linear regression model 2 (LRM2).

	Estimate	Std. Error	T value	<i>p</i> -value
Intercept	−3.6480	0.8256	−4.419	<0.0001
Wave period	1.1225	0.06405	17.526	<0.0001

Table A4. Coefficients for linear regression model 3 (LRM3).

	Estimate	Std. Error	T value	<i>p</i> -value
Intercept	−21.5779	0.2745	−78.60	<0.0001
Wave height	18.2094	0.1226	148.52	<0.0001
Wave Period	0.8152	0.0192	42.38	<0.0001

Table A5. Coefficient of linear regression model 4 (LRM4).

	Estimate	Std. Error	T value	p-value
Intercept	0.5749	0.4059	1.416	0.1568
Wave height	-1.7767	0.6169	-2.880	0.0040
(Wave height)²	7.3617	0.2159	34.104	<0.0001

Table A6. Coefficients for linear regression model 5 (LRM5).

	Estimate	Std. Error	T value	p-value
Intercept	1.7082	0.5411	3.157	0.0016
Wave height	-1.5451	0.4370	-3.536	0.0004
Wave period	-0.9920	0.0415	-23.910	2×10^{-16}
Wave height · wave period	1.520	0.0330	46.130	2×10^{-16}

Table A7. Correlogram for autocorrelation and partial autocorrelation of power.

Autocorrelation	Partial Correlation	AC	PAC	Q-Stat	Prob	
		1	0.875	0.875	1737.6	0.000
		2	0.813	0.203	3238.7	0.000
		3	0.760	0.067	4549.8	0.000
		4	0.715	0.042	5710.5	0.000
		5	0.659	-0.040	6698.8	0.000
		6	0.625	0.055	7588.2	0.000
		7	0.590	0.017	8381.4	0.000
		8	0.538	-0.082	9039.9	0.000
		9	0.493	-0.022	9593.4	0.000
		10	0.457	0.006	10069.	0.000
		11	0.430	0.037	10489.	0.000
		12	0.400	0.007	10854.	0.000
		13	0.365	-0.042	11158.	0.000
		14	0.350	0.057	11437.	0.000
		15	0.321	-0.027	11673.	0.000
		16	0.294	-0.016	11870.	0.000
		17	0.281	0.048	12051.	0.000
		18	0.265	-0.011	12212.	0.000
		19	0.253	0.027	12358.	0.000
		20	0.236	-0.014	12486.	0.000
		21	0.218	-0.030	12595.	0.000
		22	0.209	0.036	12695.	0.000
		23	0.200	0.009	12787.	0.000
		24	0.194	0.017	12873.	0.000
		25	0.187	0.001	12953.	0.000
		26	0.184	0.012	13031.	0.000
		27	0.176	0.007	13102.	0.000
		28	0.173	0.013	13171.	0.000
		29	0.163	-0.028	13232.	0.000
		30	0.161	0.022	13292.	0.000
		31	0.157	-0.000	13349.	0.000
		32	0.153	0.005	13403.	0.000
		33	0.148	0.000	13453.	0.000
		34	0.138	-0.030	13497.	0.000
		35	0.132	0.012	13537.	0.000
		36	0.128	0.010	13575.	0.000

Appendix B: residual analysis and diagnostic test for regression models.

The residuals analysis studied are linearity, normality, independence, and homoscedasticity of the error terms.

Linearity test

The residual plot from the regression models developed could be used to investigate if variables

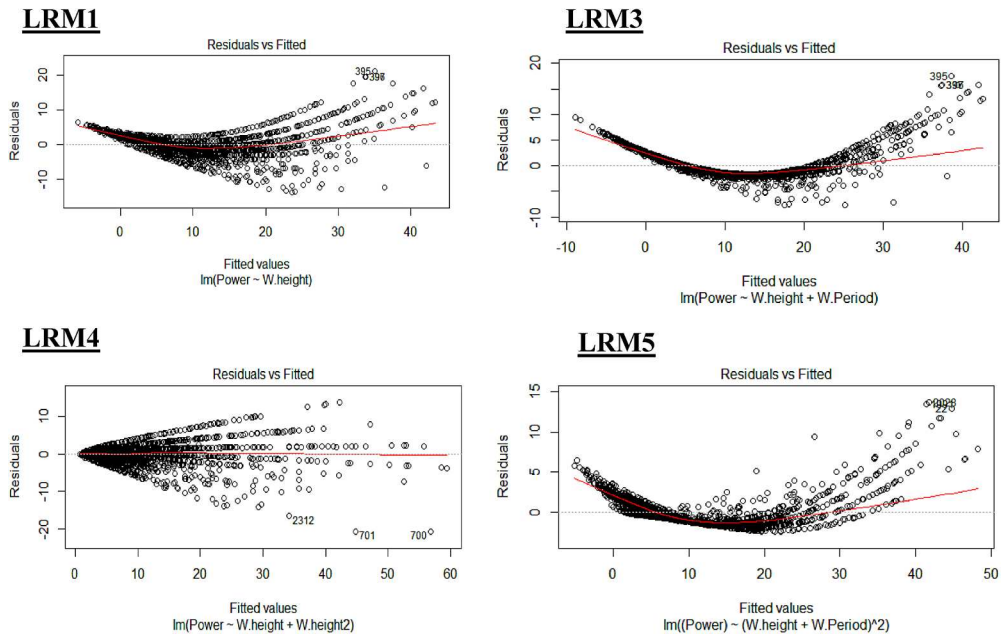


Figure B1. Plots for the Residual vs. predicted values from regression models.

have any linear relationship. If the plot is equally spread, crowding towards the central line of the plot with no overall pattern, then it is known that independent and dependent variables have a linear relationship.

Figure B1 shows the residual plots against the predicted variables from all the models, except Model 2 which gives the worst performance. The residual plots do not exhibit the properties of linearity since the residual plots are not symmetrical along the zero residual; data are not clustered along the residual zero lines, do not have a general pattern and hence they do not indicate randomness. Therefore, it can be interpreted that the independent and dependent variables do not have a linear relationship.

Normality test

Normality test is done to check if the distribution of the residuals is normal or not. Shapiro Wilk’s method and the normal Q-Q plot are used to check if the distribution is normal. Shapiro Wilk’s test statistics (W) is based on the correlation between the error and the corresponding normal score. The p and W statistics values are found using the R and are presented in Table B1 for all five models. The results reveal that the distribution of the residuals is not normal since the p -value for each model is less than 0.05.

Table B1. Shapiro-Wilk test for normality of residuals.

	<i>W</i> -value	<i>p</i> -value
Model 1	0.9303	<0.0001
Model 2	0.8510	<0.0001
Model 3	0.8341	<0.0001
Model 4	0.8701	<0.0001
Model 5	0.8123	<0.0001

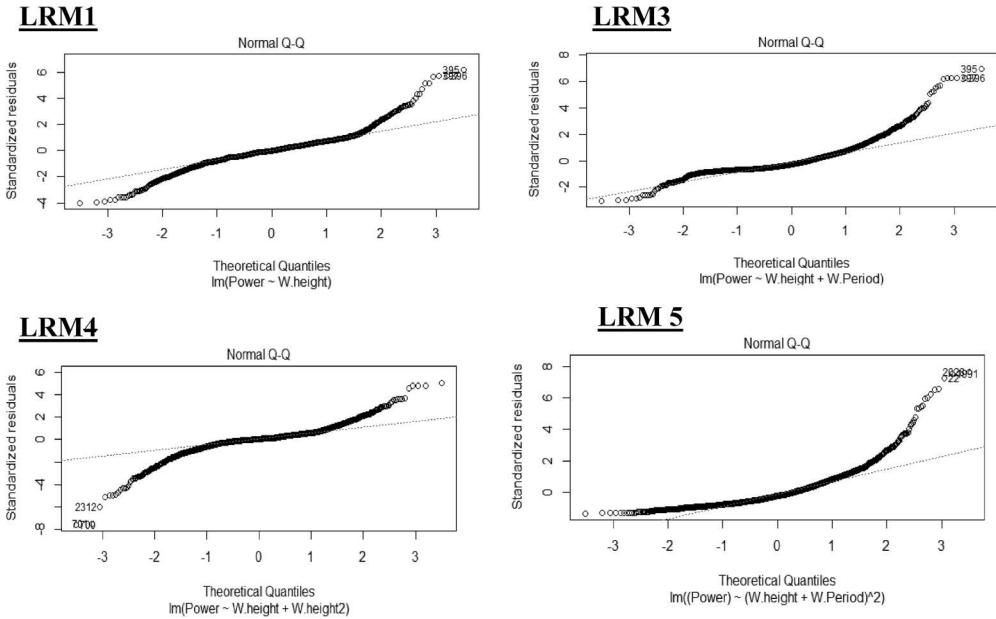


Figure B2. Normal Q-Q plot for residuals.

The normality of residuals is further studied using a Q-Q plot as shown in Figure B2 given below.

The Q-Q plot indicates the distribution is not normal since the majority of the points deviate away from the diagonal line for the models shown in Figure B2. Therefore, based on the results of Shapiro-Wilk tests and Q-Q plots, it can be conclusively said that the distribution of residuals is not normal, hence, fails to meet the assumption of normality for regression models developed.

Independence test

Multi-collinearity happens when the independent variable is highly correlated to each other. For a data set, multi-collinearity can be checked in two ways. It can be achieved by understanding the correlation table and by using the Variance Inflation Factor (VIF). The magnitude of the correlation coefficient less than 0.80 and a VIF value less than 10 implies that there is a case of multi-collinearity.

The correlation between these two independent variables was 0.0947 as discussed in Table 10. Since the value is close to zero, it can be said that the variables are not having multi-collinearity. This is also verified by looking into the variance inflation factor of 1.011679, which was found using the R software. Since VIF is less than 10, it indicates that the two independent variables show no correlation with each other. Thus, with the given VIF value and correlation value from Table 6, it can be said that it is a case of non-multi-collinearity.

Homoscedasticity

This assumption is verified using the plot of standardised residuals against the predicted values to see if points are symmetrical across the central line. If in case, the distribution displays a conic pattern, then it can be said that the data is heteroscedastic. Figure B3 displays the plots of standardised residuals against the fitted values of the models. After examining these graphs, the data is heteroscedastic and not homoscedasticity.

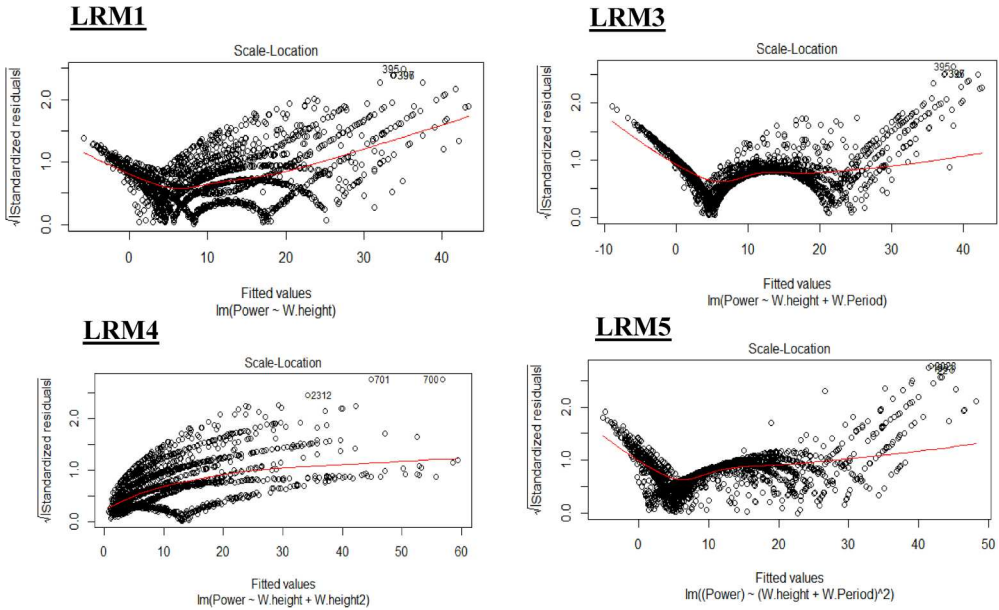


Figure B3. Examining homoscedasticity in the data.

The analyses suggests that these regression models failed to meet the linearity, independence, and normality tests, which means the linear regression models’ goodness of fit test may not be a powerful measure to consider, thus, limiting to detect the best linear fit model.

Appendix C: results of ANN models with logistics and tangent hyperbolic transfer function

Table C1. ANN results using a logistic transfer function on training data.

Model	MSE	MAE	RMSE	MAPE	R ²
ANN(2,2,1)	0.438158	0.366239	0.661935	4.712908	0.994666
ANN(2,3,1)	0.154374	0.152576	0.392905	2.44903	0.998121
ANN(2,4,1)	0.194781	0.255918	0.44134	4.681368	0.997629
ANN(2,5,1)	0.120116	0.193089	0.346577	3.942909	0.998538
ANN(2,2,2,1)	0.205027	0.311811	0.452799	6.43163	0.997504
ANN(2,2,3,1)	0.232456	0.24658	0.482137	4.088264	0.99717
ANN(2,2,4,1)	0.389426	0.369118	0.62404	5.975992	0.99526
ANN(2,2,5,1)	0.144034	0.268675	0.379519	5.719171	0.998247
ANN(2,3,2,1)	0.1851	0.23252	0.430233	4.708729	0.997747
ANN(2,4,2,1)	0.089689	0.14755	0.299481	2.674123	0.998908
ANN(2,5,2,1)	0.107043	0.233296	0.327175	5.093479	0.998697

(Continued)

Table C1. Continued.

Model	MSE	MAE	RMSE	MAPE	R ²
ANN(2,3,3,1)	0.138564	0.208951	0.372242	4.150272	0.998313
ANN(2,3,4,1)	0.113813	0.145099	0.337363	2.352499	0.998615
ANN(2,4,3,1)	0.28876	0.346976	0.537364	5.400831	0.996449
ANN(2,2,2,2,1)	0.286011	0.346002	4.980712	4.980712	0.996519
ANN(2,3,2,2,1)	0.384294	0.410553	0.619915	6.916745	0.995322
ANN(2,3,3,2,1)	0.254080	0.326123	0.504064	4.940367	0.996907
ANN(2,3,3,3,1)	0.272604	0.33867	0.522182	5.194215	0.996682

Table C2. ANN results using the tangent hyperbolic transfer function on training data.

Model	MSE	MAE	RMSE	MAPE	R ²
ANN(2,2,1)	0.346118	0.3845552	0.588318	5.786395	0.9957868
ANN(2,3,1)	0.3581068	0.3940793	0.59842	6.585868	0.9956409
ANN(2,4,1)	0.012736	0.07530997	0.112854	1.377457	0.999845
ANN(2,5,1)	0.01740737	0.08239512	0.131937	1.329459	0.9997881
ANN(2,6,1)	0.01700308	0.09917377	0.130396	2.113108	0.999793
ANN(2,7,1)	0.02586862	0.09396279	0.160837	1.778243	0.9996851
ANN(2,8,1)	0.03967738	0.1330904	0.199192	2.3356	0.999517
ANN(2,2,2,1)	0.5082552	0.4726422	0.71292	7.446726	0.9938131
ANN(2,3,2,1)	0.0121041	0.07462835	0.110019	1.342473	0.9998527
ANN(2,4,2,1)	0.02037198	0.080522	0.142731	1.534435	0.999752
ANN(2,5,2,1)	0.0153825	0.07265613	0.124026	1.325115	0.9998128
ANN(2,6,2,1)	0.01289422	0.05813862	0.113553	0.945534	0.999843
ANN(2,7,2,1)	0.007637874	0.06541977	0.087395	1.266429	0.999907
ANN(2,8,2,1)	0.01570243	0.08029146	0.125304	1.526515	0.9998089
ANN(2,9,2,1)	0.02687869	0.09342489	0.163943	1.926674	0.9996728
ANN(2,2,3,1)	0.02349837	0.1029379	0.153292	2.114319	0.999714
ANN(2,3,3,1)	0.02102271	0.09096861	0.144992	1.587052	0.9997441
ANN(2,4,3,1)	0.008928545	0.05607203	0.094491	0.829993	0.9998913
ANN(2,5,3,1)	0.02242317	0.09999282	0.149744	2.03041	0.999727
ANN(2,6,3,1)	0.0168558	0.09103077	0.12983	1.712516	0.9997948
ANN(2,7,3,1)	0.01433458	0.07726367	0.119727	1.384213	0.9998255
ANN(2,2,2,2,1)	0.34947750	0.3941856	0.591166	6.191933	0.9957459
ANN(2,3,2,2,1)	0.00837800	0.09193283	0.0998625	0.9903954	0.9998224
ANN(2,4,2,2,1)	0.2892799	0.347779	0.5378475	5.387941	0.9964787
ANN(2,3,3,2,1)	0.0125108	0.0652756	0.1118519	1.094733	0.9998477
ANN(2,3,3,3,1)	0.02048658	0.09516317	0.143131	1.494789	0.9997506